Journal of Sound and Vibration (2002) **253**(2), 485–505
doi:10.1006/jsvi.2001.4065, available online at http://www.idealibrary.com on IDEAL®

ANALYSIS OF VIBRATIONS AND ENERGY FLOWS IN SANDWICH PLATES BEARING CONCENTRATED MASSES AND SPRING-LIKE INCLUSIONS IN HEAVY FLUID-LOADING CONDITIONS

S. V. Sorokin

Department of Engineering Mechanics, State Marine Technical University of St. Petersburg, Lotsmanskaya str., #3, St. Petersburg 190008, *Russia*

(*Received* 9 *April* 2001, *and in final form* 7 *September* 2001)

Vibrations of and the energy propagation in an infinitely long fluid-loaded sandwich beam (a plate of the sandwich composition in one-dimensional cylindrical bending) bearing concentrated masses and supported by springs are described in the framework of the sixth order theory of multilayered plates coupled with the standard theory of linear acoustics. A sandwich plate is loaded by a layer of a compressible fluid which is bounded opposite to a plate side by a rigid baffle. The dispersion equation for a fluid-loaded sandwich plate is derived. The wave numbers (complex, pure real and pure imaginary) and relevant normal modes (both the travelling and the evanescent ones) are obtained. Their dependence on the parameter of a fluid's depth is studied. Then the Green matrix is constructed analytically as a linear combination of normal modes to describe the response of a plate and an acoustic medium to the point loading by a force or a moment. Continuity conditions at the loaded cross-section of a plate and in a fluid are formulated. Attention is focused at the selection of roots of the dispersion relation for the formulation of the continuity condition for a fluid at the loaded cross-section. The convergence rate of an approximate solution based on the modal composition of the Green matrix is estimated. The parametric study of the "structural" and the "fluid" energy flows in a fluid-loaded sandwich plate without inclusions is performed for various excitation conditions. Then the Green matrix method is applied to analyze the influence of a pair of identical inclusions on localization of vibrations (modal trapping) and energy flows. Conditions of localization of flexural waves at these inhomogeneities are explored.

1. INTRODUCTION

The present paper concerns several subjects each of which has received much attention in the relevant literature. These subjects are: a theory of sandwich plates, the Green functions for elastic structures in heavy fluid-loading conditions, energy transportation in coupled acoustic–elastic systems, trapped modes in unbounded waveguides. The purpose of this introduction is to discuss briefly the formulation of a problem treated here with respect to the related subjects rather than to give a detailed survey of research papers in the above areas. Therefore, references cited below are aimed to underline a novelty of the formulation which presents overlapping of these aspects.

A theory of sandwich plates suggested in reference [1] is used for the analysis of stationary vibrations in cylindrical bending and attention is focused on the comparatively low-frequency regime of motions. Then, governing differential equations of the sixth order

0022-460X/02/$35.00

may appropriately be adopted to describe dynamics of such a plate. This theory deals with dominantly flexural waves and also with dominantly shear waves which could be either of an evanescent or of a travelling kind (depending on the frequency of excitation, see references [2, 3]). It has been successfully applied to the analysis of vibrations of plates bearing concentrated masses and springs in reference [3] and to the analysis of vibrations of fluid-loaded plates in reference [4].

The Green functions of vibrations of infinitely long fluid-loaded elastic plates in cylindrical bending have been constructed, for example in references [5, 6] and problems of their forced vibrations have been thoroughly considered in references [5–8]. In all these references, a classic Kirchhoff theory is used, heavy fluid loading is produced by an unbounded volume of an acoustic medium and the acoustic emission to a far field is analyzed. However, in some applications, heavy fluid loading of an elastic structure is produced by the layer of a fluid (for example, an ice shield on a shallow water, a pipe of rectangular cross-section filled by a fluid, etc.). In such a case (which is considered in the present paper), the modal decomposition may be conveniently used to formulate the Green functions and the analysis of a dispersion equation should be employed as a necessary part of this procedure. For a purely acoustic waveguide composed by a fluid's layer of an infinite length placed between two absolutely rigid baffles, the dispersion equation has an infinite number of roots and the energy transportation is possible only at frequencies above a certain cut-on value. If an acoustic layer of a finite depth is bounded by a Kirchhoff plate at one or both sides, then the analysis of the dispersion equation for such a system suggests the absence of the cut-on frequency since the free travelling wave in a fluid-loaded plate exists in such a case [9] at an arbitrary low frequency. The relevant eigenmode may conveniently be classified as a "structure-dominated" one, whereas "fluid-dominated" modes do not propagate in this regime. As the frequency of an excitation grows, other roots of the dispersion equation become purely imaginary (space and time dependence are adopted as $\exp(kx - i\omega t)$) and "fluid-dominated" modes transform from evanescent to travelling type at a set of cut-on frequencies.

Analysis of the energy transportation in fluid-loaded Kirchhoff plates has been performed, for example, in reference [8]. A similar problem for an infinitely long cylindrical shell (Kirchhoff theory) filled by a compressible fluid has been thoroughly analyzed in references [10, 11]. The boundary integral equation method has been used in reference [12] to analyze the input mobility and the energy transmission both in a near field and in a far field in the case of mechanical excitation of such a cylindrical shell. To the best of the author's knowledge, no research has been undertaken regarding vibrations of a plate of sandwich composition in contact with the layer of an acoustic medium and energy transportation in this system.

The excitation of an infinitely long sandwich plate bearing a pair of concentrated masses supported by stiffeners may result in mode trapping between these inclusions, as is shown in reference [2]. In the present paper, the same phenomenon of trapping of flexural wave is analyzed for a sandwich plate with heavy fluid loading that also contains the aspect of novelty. This effect is analogous to the well-known phenomenon of mode trapping in purely acoustical or purely elastic waveguides, which has been thoroughly studied, for example in references [13, 14]. The localized amplification of flexural vibrations in the fluid-loaded structure may be conveniently explained in terms of energy flows in the structure and in the acoustic medium. Specifically, the trapped mode exists when a short circuit of the energy flows is developed in a certain region of the fluid-loaded structure (i.e., when the energy flows are directed opposite to each other in the structure and in the fluid). Finally, it should be pointed out, that the classical formulation of the trapped mode problem is relevant to an interaction between inclusions and a travelling incident wave coming from infinity, but from

a practical viewpoint it is probably more relevant to specify excitation conditions in terms of an external loading. A case of most interest is then the forced vibrations of an infinitely long plate loaded by a concentrated force or moment and bearing concentrated inclusions. Then, the Green function method [2, 3] appears to be a convenient tool for solving this problem since the Green matrix is available in a simple analytical form.

2. THE DISPERSION EQUATION AND NORMAL WAVES FOR A FLUID-LOADED SANDWICH PLATE

The theory of a sandwich beam is taken the form suggested in reference [1] and used in references [2–4]. The element of a sandwich beam consists of two symmetrical relatively thin, stiff skin plies and a thick, soft core ply. Dimensionless parameters are introduced to describe the internal structure of the sandwich plate: $\varepsilon = h_{skin}/h_{core}$ as a thickness parameter (a ratio of a thickness of each individual skin ply to a thickness of the core ply), $\delta = \rho_{core}/\rho_{skin}$ as a density parameter, $\gamma = E_{core}/E_{skin}$ as a longitudinal stiffness parameter and $\gamma_g = G_{core}/G_{skin}$ as a shear stiffness parameter. Hereafter, subscripts denoting parameters of skin plies are omitted. The deformation of a sandwich beam element is governed by two independent variables: a displacement of the mid-surface of the whole element w (which is the same for all plies) and a shear angle between the mid-surfaces of skin plies θ.

Details of derivation of differential equations of motions of a sandwich plate may be found in references [2–4]. Equations of motion of a fluid-loaded plate are formulated as

$$D_1 w^{\mathrm{IV}} - \Gamma(\theta' + w'') + m\ddot{w} - I_1 \ddot{w}'' = q_w + p, \tag{1a}$$

$$- D_2 \theta'' + \Gamma(\theta + w') + I_2 \ddot{\theta} = q_\theta. \tag{1b}$$

Here, q_w is the intensity of a distributed lateral force, q_θ is the intensity of a distributed shear moment and p is the contact acoustic pressure. The elastic parameters in equations (1a, b) are ($E = E_{skin}$, $h = h_{skin}$)

$$D_1 = \frac{Eh^3}{12(1-\nu^2)}\left(2 + \frac{\gamma}{\varepsilon^3}\right), \qquad D_2 = \frac{Eh^3}{2(1-\nu^2)}\left(1 + \frac{1}{\varepsilon}\right)^2,$$

$$\Gamma = \frac{Eh}{2(1+\nu)}\left(1 + \frac{1}{\varepsilon}\right)^2 \gamma_g \varepsilon, \qquad m = \rho h\left(2 + \frac{\delta}{\varepsilon}\right),$$

$$I_1 = \frac{\rho h^3}{12}\left(2 + \frac{\delta}{\varepsilon^3}\right), \qquad I_2 = \frac{\rho h^3}{2}\left(1 + \frac{1}{\varepsilon}\right)^2. \tag{1c}$$

The Poisson's ratio ν is assumed to be the same for all plies. The moments and forces are related to a lateral displacement and a shear angle as

$$M_1 = - D_1 w'', \qquad M_2 = D_2 \theta', \qquad Q = \Gamma(\theta + w'). \tag{1d}$$

Typical values of the material parameters for skin and core plies may be found in references [2–4] or in reference [15, chapter 1]. The theory of bending of sandwich beams described here is a generalization of classic Timoshenko theory [16] and the vector of generalized displacements has three components (w, w', θ). In the case of a static deformation, this theory results in equations of equilibrium identical to those given in reference [17, chapter 3].

Dynamics of an acoustic medium is governed by a wave equation for a velocity potential

$$\frac{\partial^2 \varphi}{\partial x^2} + \frac{\partial^2 \varphi}{\partial z^2} - \frac{1}{c_{fl}^2}\frac{\partial^2 \varphi}{\partial t^2} = 0, \tag{2}$$

with a continuity condition at the fluid–structure interface, $z = 0$

$$\partial\varphi/\partial z = \partial w/\partial t. \tag{3}$$

The second condition at $z = -H$ (H is the depth of the layer of an acoustic medium) is

$$\partial\varphi/\partial z = 0. \tag{4}$$

The acoustic pressure is formulated as

$$p = -\rho_{fl}\frac{\partial\varphi}{\partial t}. \tag{5}$$

For definiteness, a sandwich structure composed of isotropic individual layers is considered, so that $\gamma = \gamma_g$ and equations (1a, b) become (here $q_w = q_\theta = 0$)

$$\frac{Eh^3}{12(1-\nu^2)}\left(2+\frac{\gamma}{\varepsilon^3}\right)w'''' - \frac{Eh}{2(1+\nu)}\left(1+\frac{1}{\varepsilon}\right)^2\varepsilon\gamma(\theta'+w'') + \rho h\left(2+\frac{\delta}{\varepsilon}\right)\ddot{w} - \frac{\rho h^3}{12}\left(2+\frac{\delta}{\varepsilon^3}\right)\ddot{w}'' = p, \tag{6a}$$

$$-\frac{Eh^3}{2(1-\nu^2)}\theta'' + \frac{Eh}{2(1+\nu)}\varepsilon\gamma(\theta+w') + \frac{\rho h^3}{2}\ddot{\theta} = 0. \tag{6b}$$

To construct the Green functions for vibrations of an infinitely long sandwich beam, it is necessary to obtain the dispersion relation and formulate waves existing in an unbounded structure. The loading terms in equations (6a, b) are then set to zero, and a solution is sought in the form

$$w = A\exp(kx - \mathrm{i}\omega t), \qquad \theta = B\exp(kx - \mathrm{i}\omega t), \qquad \varphi = C(z)\exp(kx - \mathrm{i}\omega t), \tag{7a–c}$$

Standard algebra gives the following set of homogeneous algebraic equations:

$$\left[\frac{Eh^3(2+\gamma/\varepsilon^3)}{12(1-\nu^2)}k^4 - \frac{Eh\gamma\varepsilon(1+1/\varepsilon)^2k^2}{2(1+\nu)} + \frac{\rho\omega^2h^3}{12}\left(2+\frac{\delta}{\varepsilon^3}\right)k^2 - \rho h\omega^2\left(2+\frac{\delta}{\varepsilon}\right) + \rho_{fl}\omega^2\frac{\cot(H\sqrt{k^2+\omega^2/c_{fl}^2})}{\sqrt{k^2+\omega^2/c_{fl}^2}}\right]A - \frac{\gamma\varepsilon(1+1/\varepsilon)^2k}{2(1+\nu)}B = 0, \tag{8a}$$

$$\frac{Eh\gamma\varepsilon k}{2(1+\nu)}A + \left[-\frac{Eh^3k^2}{2(1-\nu^2)} + \frac{Eh\gamma\varepsilon}{2(1+\nu)} - \frac{\rho h^3\omega^2}{2}\right]B = 0 \tag{8b}$$

and upon setting the determinant of this system of algebraic equations to zero, the dispersion equation is obtained in a non-dimensional form.

$$\left[\left(2+\frac{\gamma}{\varepsilon^3}\right)K^4 - 6(1-\nu)\left(1+\frac{1}{\varepsilon}\right)^2\gamma\varepsilon K^2 + \left(2+\frac{\delta}{\varepsilon^3}\right)K^2\Omega^2 - 12\left(2+\frac{\delta}{\varepsilon}\right)\Omega^2 + 12\frac{\rho_{fl}}{\rho}\Omega^2\frac{\cot(H/h\sqrt{K^2+c^2/c_{fl}^2\Omega^2})}{\sqrt{K^2+c^2/c_{fl}^2\Omega^2}}\right][K^2-(1-\nu)\gamma\varepsilon+\Omega^2] - 6(1-\nu)^2\left(1+\frac{1}{\varepsilon}\right)^2(\gamma\varepsilon K)^2 = 0, \tag{9}$$

where $K = kh$, $\Omega = \omega h/c$, $c = \sqrt{E/\rho(1-\nu^2)}$.

Apparently, for a given frequency parameter Ω, dispersion equation (9) has infinitely many roots. An arbitrarily large number of them may be found numerically as is described, for example, in reference [10]. However, it is more convenient to expand the fluid-loading term into power series and reduce equation (9) to the polynomial form. Its order is defined by a chosen approximation level. Then, all the roots of the approximate polynomial dispersion equation are easily found by using some symbolic manipulator, see, e.g., *Mathematica* [18]. These roots must be checked as to whether they fulfil original equation (9). Further selection of the roots is based on the formulation of the Sommerfeld radiation condition at infinity for purely imaginary roots and the decay condition for complex roots, i.e., $\mathrm{Re}(K_m) < 0$, or, if $\mathrm{Re}(K_m) = 0$, then $\mathrm{Im}(K_m) > 0$. This latter choice is dictated by the selection of time dependence as $\exp(-\mathrm{i}\,\omega t)$, to ensure that the phase velocity of propagating waves is directed away from a source of the excitation.

Since the location of roots of the dispersion equation controls formulation of the Green matrix of a fluid-loaded sandwich plate, it is relevant to explore the influence of some parameters, in particular, the depth of the fluid's layer on the shape of dispersion curves $K_m(\Omega)$. An analysis of dispersion relations in purely acoustical waveguides or in purely elastic waveguides is available in most of the textbooks on dynamics. These is also a comprehensive literature related to analysis of dispersion relations in Kirchhoff plates and shells with heavy fluid loading, see, for example references [7, 9]. However, to the best of the author's knowledge, a similar analysis has not yet been performed for a sandwich plate loaded by a layer of an acoustic medium. For definiteness, the following parameters of a sandwich plate composition are specified: $\varepsilon = 0{\cdot}25$, $\gamma = 0{\cdot}0001$, $\delta = 0{\cdot}1$, $\nu = 0{\cdot}3$. This combination of parameters is typical of a plate of a naval structure made of thin steel skins and PVC core [15]. This plate is loaded by water, so that $\bar{\rho} = \rho_{fluid}/\rho = 0{\cdot}128$ and $\beta = c/c_{fluid} = 3{\cdot}258$. It is necessary to explore the roles of the frequency parameter $\Omega = \omega h/c$ and the "depth" parameter $\chi = H/h$ on the shape and location of dispersion curves. For a plate without fluid loading, dispersion curves $K_m(\Omega)$ have been presented in references [2, 3]. As follows from the results reported in these references, if the parameters of a sandwich plate composition are selected as given above, then a minimal wave length at the frequency of $\Omega = 0{\cdot}01$ is about 8 times larger, than the thickness of the whole set of three plies. Thus, it is reasonable to fix the frequency parameter at this value and to look at the influence of the depth parameter only. It is illustrated in Figure 1(a–c), where dispersion curves $K_m(\chi)$ are sketched for the range of the depth parameter $2{\cdot}5 < \chi < 50$. In Figure 1(a), real parts of roots of the dispersion equation are shown versus this parameter, whereas in Figure 1(b) a dependence of imaginary parts of complex conjugate roots is displayed. Curve A in Figure 1(b) displays a dependence of the purely imaginary wave number of "structure-dominated" mode on the parameter χ. Finally, in Figure 1(c), a dependence of the remaining two purely imaginary roots of the dispersion equation on the depth parameter is shown. The dot at the vertical axis in Figure 1(a) designates a single purely real root $K_1 = -0{\cdot}1958$ for a sandwich plate without fluid loading; two purely imaginary roots in this case are $K_2 = 0{\cdot}00908\mathrm{i}$ and $K_3 = 0{\cdot}1935\mathrm{i}$. They are designated by dots at the vertical axis in Figures 1(b, c) respectively.

Inspection of the fluid-loading term in equation (9) suggests, that in contrast to the case of an unbounded volume of a fluid in contact with a plate, a layer of the depth H produces the effect of an added stiffness, rather than effects of an added mass or of a radiation damping until the following condition holds true: $\chi\sqrt{K^2 + \beta^2\Omega^2} > \pi/2$. The case of a very small depth of a layer of an acoustic medium is not of much practical relevance, since the model of an ideal inviscid fluid probably is not valid then. Formally, a solution of the dispersion equation in this limit gives two purely imaginary roots and a pair of complex conjugate roots. All these roots are not shown in Figure 1(a–c) for $0 < \chi < 2{\cdot}5$. It should be pointed

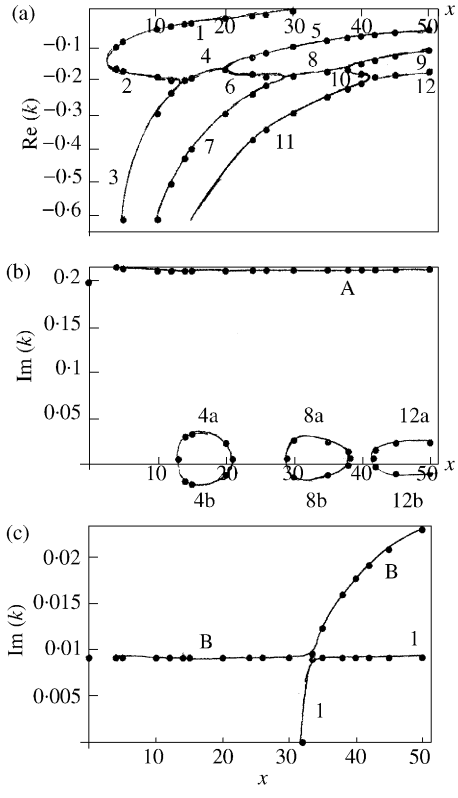

Figure 1. Dispersion curves versus depth parameter χ at $\Omega = 0{\cdot}01$: (a) real parts of complex conjugate roots; (b) imaginary parts of complex conjugate roots and a purely imaginary root; and (c) two purely imaginary roots.

out that the absolute value of complex conjugate roots decays very rapidly with a growth in the depth parameter. As the depth parameter reaches the value of $\chi \approx 2{\cdot}6$, this pair of roots becomes purely real and one of them grows as shown by curve 1 in Figure 1(a). Another one decays (see branch 2) until it matches growing purely real branch 3 at $\chi \approx 12{\cdot}5$. Branches 2 and 3 do not intersect, but leave the real axis and become the complex conjugate pair of roots with the real part plotted as curve 4 in Figure 1(a). Their imaginary parts are plotted as curves 4(a) and 4(b) in Figure 1(b). At $\chi \approx 20$, they return to the real axis and split into growing branch 5 and decaying branch 6. The latter one matches branch 7 at $\chi \approx 30$ and both real roots acquire imaginary parts shown in Figure 1(b) as curves 8(a) and 8(b). Their real part is displayed by curve 8. This scenario is repeated at the points $\chi \approx 39$ (complex conjugate roots are split into branches 9 and 10), $\chi \approx 41$ (purely real roots 10 and 11 merge and transform to the pair of complex conjugate roots 12, 12(a), 12(b) and so on to the right in Figure 1(a). Curve 1 in Figure 1(a) reaches zero at $\chi \approx 32$ and transforms to purely imaginary branch 1 in Figure 1(c). This is the first "cut-on" depth parameter at the given frequency of $\Omega = 0{\cdot}01$. Physically, it simply means that an acoustically dominated mode has transformed from the evanescent to the propagating type. Branch 1 grows very fast until it reaches another purely imaginary branch B at $\chi \approx 32{\cdot}5$. Similar to the cases described in reference [10], these branches do not intersect each other. A growth in the absolute value of the "fluid-dominated" wave number stops, whereas the absolute value of the "structure-dominated" wave number begins to grow rapidly; see Figure 1(c).

The graphs in Figures 1(a–c) are not extended to larger values of the depth parameter since all the characteristic features of dispersion curves are adequately described for $\chi < 50$.

The second and the third "cut-on" values of the depth parameter are $\chi \approx 127$ and 240. It is interesting to note that cut-on depth parameters for a layer of an acoustic medium between two absolutely rigid walls at the same frequency found from an elementary formula $\chi_m = m\pi/2\beta\Omega$, $m = 1, 3, 5, \ldots$ are $\chi_1 = 48{\cdot}2$, $\chi_2 = 144{\cdot}6$, $\chi_3 = 241$. As is seen, the third "cut-on" value of the depth parameter is adequately predicted by use of this simplified model. This result is in perfect agreement with well-known results reported for other fluid-loaded elastic structures, for example, for a fluid-loaded cylindrical shell; see references [10, 11]. It is not necessary to continue analysis for other values of the frequency parameter, since the pattern of dispersion curves $K_m(\chi)$ remains the same with the whole set of curves just shifted towards larger values of the parameter χ when the frequency parameter Ω diminishes and in the opposite direction when it grows.

For each root K_m, a modal coefficient is found from equation (8b) as

$$B_m = \frac{(1-\nu)\varepsilon\gamma K_m}{K_m^2 - (1-\nu)\varepsilon\gamma + \Omega^2} \tag{10}$$

and a function $C_m(z)$ is introduced as

$$C_m(z) = \frac{\Omega}{\sqrt{K_m^2 + \beta^2\Omega^2}} \frac{\exp(\mathrm{i}\bar{z}\sqrt{K_m^2 + \beta^2\Omega^2}) + \exp(-\mathrm{i}(z/H + 2\chi)\sqrt{K_m^2 + \beta^2\Omega^2})}{1 - \exp(-2\mathrm{i}\chi\sqrt{K_m^2 + \beta^2\Omega^2})}. \tag{11}$$

Then, formulas (10, 11) define for each K_m a wave which either travels from the left to the right or decays in this direction.

3. THE GREEN MATRIX FOR A FLUID-LOADED SANDWICH PLATE

To perform the analysis of forced vibrations of a fluid-loaded sandwich plate, the Green matrix should be constructed. The elements of this matrix are easy to derive since the roots of the dispersion polynomial and the modal coefficients are readily available. They are composed as linear combinations of the normal modes for the "fundamental" loading cases at an arbitrary cross-section $x = \xi$ of a fluid-loaded sandwich plate. Unlike the case of a sandwich plate without fluid loading treated in references [2, 3], the loading conditions should contain a "fluid" part.

For a unit transverse force acting at $x = \xi$, the first condition formulates a unit jump in its value

$$\Gamma\left[\Theta_1(x,\xi) + \frac{\partial W_1(x,\xi)}{\partial x}\right] - D_1\frac{\partial^3 W_1(x,\xi)}{\partial x^3} - I_1\omega^2\frac{\partial W_1(x,\xi)}{\partial x} = \frac{1}{2}\operatorname{sign}(x-\xi). \tag{12a}$$

The second condition is related to the symmetry of a flexural deflection with respect to the loaded cross-section:

$$\partial W_1(x,\xi)/\partial x = 0. \tag{12b}$$

The symmetry condition is also formulated for a shear angle

$$\Theta_1(x,\xi) = 0. \tag{12c}$$

The fluid velocity field produced by a transverse force acting at an infinitely long sandwich plate should also be symmetrical with respect to the cross-section $x = \xi$, e.g.,

$$\partial\varphi_1/\partial x = 0. \tag{12d}$$

This condition should hold at any point $-H < z < 0$.

A set of normal modes is substituted into equations (12),

$$W_1(|x-\xi|) = h \sum_{m=1}^{M} \bar{W}_m \exp(K_m|x-\xi|),$$

$$\Theta_1(|x-\xi|) = \sum_{m=1}^{M} B_m \bar{W}_m \operatorname{sign}(x-\xi) \exp(K_m|x-\xi|),$$

$$\varphi_1(|x-\xi|, z) = -hc \sum_{m=1}^{M} C_m(z) \bar{W}_m \exp(K_m|x-\xi|) \tag{13}$$

and three linear algebraic equations containing unknown coefficients $\bar{W}_m$, $m = 1, \ldots, M$ are obtained:

$$\sum_{m=1}^{M} \left[\Gamma(\beta_m + K_m) - \frac{D_1}{h^2} K_m^3 - I_1 \omega^2 K_m \right] \bar{W}_{1m} = \frac{1}{2}, \tag{14a}$$

$$\sum_{m=1}^{M} K_m \bar{W}_{1m} = 0, \qquad \sum_{m=1}^{M} \beta_m \bar{W}_{1m} = 0. \tag{14b, c}$$

This system is underdetermined, but it is necessary to also fulfil condition (12d) in a fluid at $x = \xi$. This continuity condition may be fulfilled only in the average sense and the exact formulation of the Green matrix may be obtained in expansion on the normal modes when $M \to \infty$. In practical computations, a few terms in equations (13) can be retained so that the Green matrix is constructed in an approximate manner, but the accuracy may always be assessed by adding extra terms in expansions (13). The derivative of a velocity potential is

$$\frac{\partial \varphi}{\partial x} = -c \sum_{m=1}^{M} \bar{W}_m \frac{\Omega}{\sqrt{K_m^2 + \beta^2 \Omega^2}} \frac{\exp(\mathrm{i}(z/H)\sqrt{K_m^2 + \beta^2 \Omega^2}) + \exp(-\mathrm{i}(z/H + 2\chi)\sqrt{K_m^2 + \beta^2 \Omega^2})}{1 - \exp(-2\mathrm{i}\chi\sqrt{K_m^2 + \beta^2 \Omega^2})}.$$

The Galerkin orthogonolization technique is used for "condensation" of the continuous "fluid" boundary condition (12d):

$$\int_{-H}^{0} \sum_{m=1}^{M} \bar{W}_m K_m C_m(z) C_j(z) \, \mathrm{d}z = 0, \quad j = 4, 5, \ldots, M. \tag{14d}$$

Equation (14d) is formulated for "extra" roots of dispersion equation, which originated from the fluid-loading term in equation (9). In selection of these roots, it is necessary to address the analysis of dispersion curves. The "structure-dominated roots" are those designated by curve 1 in Figure 1(a), and curve A in Figure 3(b) and curve B in Figure 3(c) of section 4. Respectively, all other roots should be attributed to the "fluid-dominated modes".

Naturally, an extension of system (14) by adding one more root results in modification of values of the modal coefficients found in a previous approximation. This gives a convenient tool to judge the accuracy and the convergence rate of this algorithm. A brief analysis of this issue has been performed for the set of parameters given above. Convergence has been checked in direct comparison of values of the modal coefficients found in subsequent approximations. Another way to check the validity of subsequent approximations is related to a comparison of the input power with the energy flows in the structure and in the acoustic medium (the check of the energy conservation), which will be discussed in detail in the next section of the paper. A tolerance level of 1% has been reached with five modes retained in computations in the range $3{\cdot}8 < \chi < 12$ of the depth parameter. In the range $12 < \chi < 21$, it is necessary to keep the six first modes, in the range $21 < \chi < 39$ as the number of modes increases to seven. It remains the same in the range $39 < \chi < 41$, but in the range $41 < \chi < 50$ it is necessary to keep eight modes. Summing up the results of computations, it

may be concluded that besides all propagating modes, in the formulation of condition (14d) it is necessary to include all evanescent modes up to a pair of those relevant to complex conjugate roots of the dispersion equation (9) plus the next one. If the dispersion equation only has either purely real or purely imaginary roots, then their number should not be less than the number of modes retained in the analysis at the previous step (in terms of progressing from smaller values of the parameter χ to its larger values). As is seen from Figure 1(a), multiple branching of dispersion curves makes it necessary to keep a substantial amount of terms in expansion (13) to deal with the high-frequency excitation of a plate in contact with a sufficiently thick layer of an acoustic medium. Hence, in the limiting case of an unbounded volume, i.e., when $\chi \to \infty$, summation on modes should be replaced by integration and the problem of formulation of the Green matrix should be solved in terms of integral transformations; see references [5–9] for the case of a Kirchhoff's plate.

The energy transportation is associated only with purely propagating modes and a far field is actually composed only of the modes of this type. The contribution of the evanescent modes is important only in some vicinity of the loading point and decays at a rather short distance from this point. However, the correct formulation of a near field is very important because it defines the input mobility of the fluid-loaded plate. Insufficient accuracy in fulfilment of boundary condition (14d) also results in violation of the energy conservation law and in an incorrect formulation of a near field.

To complete the formulation of the Green matrix of a fluid-loaded sandwich plate, two other "fundamental" cases should be considered: loading by a unit bending moment and loading by a unit shear moment. In the former case, the "structural" loading conditions at $x = \xi$ are

$$D_1 \frac{\partial^2 W_2(x, \xi)}{\partial x^2} = \frac{1}{2} \operatorname{sign}(x - \xi), \qquad W_2(x, \xi) = 0, \qquad \frac{\partial \Theta_2(x, \xi)}{\partial x} = 0. \tag{15a–c}$$

The first one formulates a unit jump in a bending moment at the loaded cross-section, the second one is related to the absence of a lateral displacement at $x = \xi$ and the last one formulates the absence of any jump in a shear moment. Apparently, in this case the plate's deformation is skew-symmetric with respect to the loaded cross-section $x = \xi$. The Fluid velocity field produced by a unit bending moment acting at an infinitely long sandwich plate should also be skew-symmetrical, i.e.,

$$\varphi_2 = 0. \tag{15d}$$

This condition should hold at any point $-H < z < 0$.

A set of the normal modes is substituted into equations (15),

$$W_2(|x - \xi|) = h \sum_{m=1}^{M} \bar{W}_{2m} \operatorname{sign}(x - \xi) \exp(K_m |x - \xi|), \tag{16a}$$

$$\Theta_2(|x - \xi|) = \sum_{m=1}^{M} B_m \bar{W}_{2m} \exp(K_m |x - \xi|), \tag{16b}$$

$$\varphi_2(|x - \xi|, z) = -hc \sum_{m=1}^{M} C_m(z)\, \bar{W}_{2m} \operatorname{sign}(x - \xi) \exp(K_m |x - \xi|) \tag{16c}$$

and one obtains the following system of linear algebraic equations:

$$\sum_{m=1}^{M} \frac{D_1}{h^2} K_m^2\, \bar{W}_{2m} = \frac{1}{2}, \qquad \sum_{m=1}^{M} \bar{W}_{2m} = 0, \qquad \sum_{m=1}^{M} B_m K_m\, \bar{W}_{2m} = 0, \tag{17a–c}$$

$$\int_{-H}^{0} \sum_{m=1}^{M} \bar{W}_{2m} C_m(z) C_j(z)\, \mathrm{d}z = 0, \quad j = 4, 5, \ldots, M. \tag{17d}$$

The last loading case is formulated as

$$\frac{\partial^2 W_3(x, \xi)}{\partial x^2} = 0, \qquad W_3(x, \xi) = 0, \tag{18a, b}$$

$$D_2 \frac{\partial \Theta_3(x, \xi)}{\partial x} = -\frac{1}{2} \operatorname{sign}(x - \xi), \qquad \varphi_3(x, \xi, z) = 0, \ -H < z < 0. \tag{18c, d}$$

Standard substitution of formulas (16) into this set of conditions gives

$$\sum_{m=1}^{M} K_m^2 \bar{W}_{3m} = 0, \qquad \sum_{m=1}^{M} \bar{W}_{3m} = 0, \qquad D_2 \sum_{m=1}^{M} B_m K_m \bar{W}_{3m} = \frac{1}{2}, \tag{19a–c}$$

$$\int_{-H}^{0} \sum_{m=1}^{M} \bar{W}_{3m} C_m(z) C_j(z)\, \mathrm{d}z = 0, \quad j = 4, 5, \ldots, M. \tag{19d}$$

A solution of these systems uniquely defines all elements of the Green matrix of vibrations of a fluid-loaded sandwich plate. The Green matrix is directly applicable to the analysis of vibrations of an infinitely long beam of sandwich composition, as it is formulated with the Sommerfeld condition and the loading conditions already taken into account.

4. ENERGY FLOWS IN AN INFINITELY LONG HOMOGENEOUS FLUID-LOADED SANDWICH PLATE DRIVEN BY A TRANSVERSE FORCE, BY A BENDING MOMENT OR BY A SHEAR MOMENT

The formulation of the Green matrix given in the previous section permits one to compute easily the input mobility of a homogeneous plate and to compare the energy flows through the structure and through the acoustic medium in various excitation conditions. Since stationary vibrations are considered, only energy flows averaged over a period are discussed hereafter. The energy flow in a sandwich plate is defined as

$$N_{plate}(x) = \frac{1}{2} \operatorname{Re}[Q(x)\hat{v}(x) - M_1(x)\hat{v}'(x) - M_2(x)\hat{\vartheta}(x)]. \tag{20a}$$

In formula (20a), $v(x) = -\mathrm{i}\omega w(x)$ and $\vartheta(x) = -\mathrm{i}\omega\theta(x)$ are velocities of an element of the plate in its lateral and in-plane shear motions, and $\hat{v}(x)$, $\hat{\vartheta}(x)$ are their complex conjugates. The energy flow in an acoustic medium is

$$N_{fluid}(x) = \frac{1}{2} \int_{-H}^{0} p(x, z)\bar{v}_x(x, z)\, \mathrm{d}z. \tag{20b}$$

In formula (20), $\hat{v}_x(x, t)$ is a complex conjugate of the axial component of the fluid velocity. Finally, the input power is formulated as

$$N_{input} = \frac{1}{2} \operatorname{Re}[Q(\xi)\hat{v}(\xi) - M_1(\xi)\hat{v}'(\xi) - M_2(\xi)\hat{\theta}'(\xi)]. \tag{20c}$$

In equation (20c), ξ is a co-ordinate of the loading point.

The energy balance (the conservation law) gives the apparent relation between these three quantities to be held at an arbitrary cross-section of the plate $x = Const$,

$$N_{plate}(x) + N_{fluid}(x) = N_{input}. \tag{21}$$

For convenience, hereafter a non-dimensional power per unit width is introduced as $\bar{N} = N/\rho hc^3$. From a practical viewpoint, the energy transportation in fluid-loaded structures is an important issue in various applications, such as, for example, propagation of noise and vibrations in floating plates and fluid-filled pipelines. Then, two aspects should be discussed in detail. The first one is the distribution of the energy flow between the "structural path" and the "fluid path" in a far field, the second one is the energy exchanges in a near field. It should be pointed out that the Green functions technique is a tool equally applicable for the analysis a near field and a far field. In a near field, the energy put into the fluid-loaded structure by purely mechanical excitation is partly transmitted to the fluid. Typically, some fluctuations in the amounts of energy distributed between the fluid and the structure occur at a certain distance from the excitation point. The transition from a near field to a far field is associated with the onset of a balance between the amounts of energy transported by the "fluid path" and by the "structural path". This is an important issue since different devices are used to suppress the propagation of a fluid and a structure-borne sound.

The parameters of a water-loaded sandwich plate composition are specified as before, i.e., $\gamma = 0{\cdot}0001$, $\delta = 0{\cdot}1$, $\varepsilon = 0{\cdot}25$, $\nu = 0{\cdot}3$ and some computations are carried out for this plate. The relatively high-frequency excitation $\Omega = 0{\cdot}01$ is considered first. The analysis of dispersion curves $K_m(\chi)$ at this frequency suggests several qualitatively different cases to be explored. The first one is relevant to the thickness of a fluid layer taken as $\chi = 10$. The energy flows from the excitation point to the right in the plate and in the fluid are displayed in Figure 2(a) by curves 1 and 2 respectively. The upper straight lines gives a half of the energy input produced by the concentrated force. Evidently, due to the symmetry of excitation conditions, the power input is equally distributed among the left and the right parts of the plate. As follows from the analysis of dispersion curves, in this case no propagating "fluid-dominated" modes exist, so that the energy transportation in the fluid layer is fairly small and it is associated with the "structure-dominated" modes. This graph suggests the clear interpretation of nearfield and farfield zones regarding the energy transportation. There is a re-distribution of the energy between the structure and the fluid in a near field, whereas proportion of the energy carried by the structure and by the fluid is held fixed in a far field. A near field is located in the vicinity of the excitation point, e.g., $|x| < 70\,h$ in this case. Very close to the loading point, the energy is "dropped" from the plate to the acoustic medium, but at a short distance from this zone it is returned back to the structure (see curves 1 and 2). It is also interesting to note that there is a small region in the fluid-loaded plate where the energy flow in the structure slightly exceeds the input power. This does not violate the energy conservation law since the energy flow in a fluid is negative; see curve 2. Such a localized energy short circuit indicates the amplification of structural vibrations. The next case illustrated by Figure 2(b) is $\chi = 30$, when the wave number of one of the "fluid-dominated" modes is still purely real and negative, but its magnitude is very small. Curves 1 and 2 display a dependence of structural and fluid energy flows, respectively, on a distance from the excitation point. In contrast to the previous case, a near field is spread over a much larger distance. It is also remarkable that the energy flow in an acoustic medium is negative in many places, indicating the presence of multiple loops of the energy circulation. A decay in the amplitudes of fluctuations is clearly observed in Figure 2(b). Thus, the energy distribution between the plate and the fluid becomes constant, but this balance is established sufficiently far from the excitation point. Most of the energy in the far field is transported through the structure. The last case is $\chi = 50$, when the depth parameter is well above its first cut-on value. As is seen in Figure 2(c), the energy flow is distributed between the fluid and the structure approximately in proportion 1/4 (in an averaged sense), i.e., unlike the previous two cases, a considerable amount of the energy is transported by the

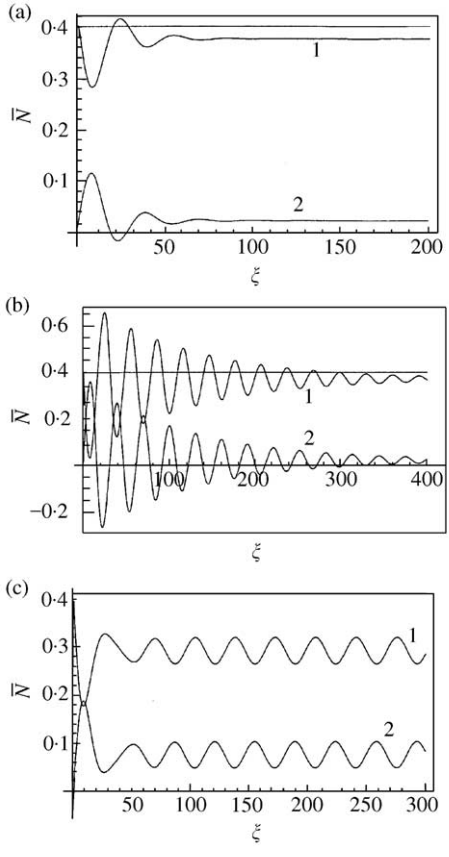

Figure 2. Energy flows in a homogeneous plate loaded by a transverse force at $\Omega = 0{\cdot}01$: (a) $\chi = 10$; (b) $\chi = 30$; and (c) $\chi = 50$.

acoustic medium. Another distinctive feature of this graph is the steady fluctuation of the energy flows in the structure and in the fluid which of course preserves overall energy balance (21).

Graphs similar to those in Figure 2 are easily obtained for larger values of the depth parameter (e.g., $\chi = 100$) and lower frequencies (e.g., $\Omega = 0{\cdot}0001$) with other parameters kept the same as before. In this case, the energy flows in the plate and in the fluid from the excitation point to the right are displayed in Figure 3 by curves 1 and 2 respectively. The upper straight line gives a half of the energy input by a concentrated force. This graph has the same features as the graph displayed in Figure 2(a), but an amount of the energy transported in the fluid is not much less than an amount of the energy transported in the structure. This may be explained simply by an increase in "capacity" of the fluid path with a growth in the depth parameter.

Now, we briefly address the loading of an infinitely long sandwich plate by a unit concentrated bending moment and by a unit concentrated shear moment. All parameters of the sandwich composition are the same as before. In Figure 4(a, b), the energy flow is plotted versus a distance from the excitation point for the case of a unit bending moment. The frequency parameter is $\Omega = 0{\cdot}01$, the depth parameter is $\chi = 10$ and 50 respectively. The magnitude of the power input is considerably smaller, than in the previous case of the excitation by a unit lateral force, but a distribution of the energy between the structure and

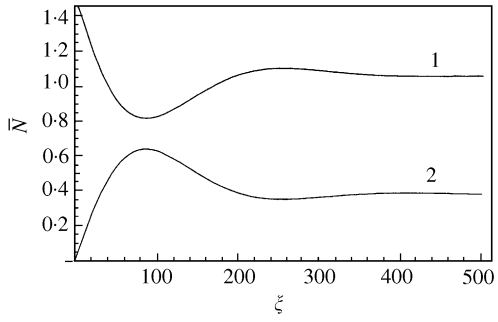

Figure 3. Energy flows in a homogeneous plate at $\Omega = 0{\cdot}001$, $\chi = 100$.

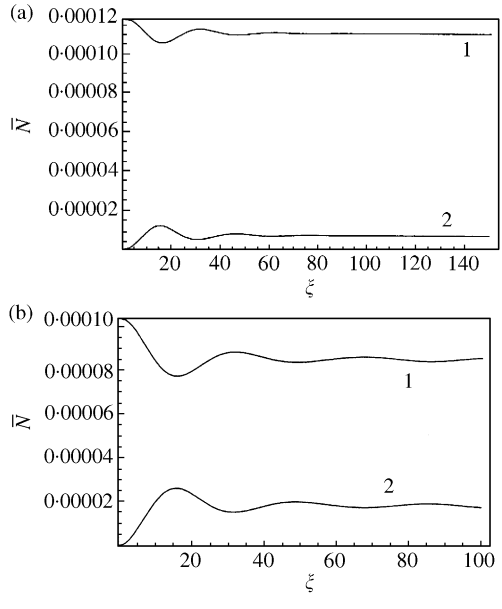

Figure 4. Energy flows in a homogeneous plate loaded by a bending moment $\Omega = 0{\cdot}01$: (a) $\chi = 10$; and (b) $\chi = 50$.

the fluid is qualitatively the same as shown in Figure 2(a, c). There is also a fluctuation in this distribution in the case, when the depth parameters exceed the first cut-on value, but its amplitude is much smaller than in the previous case. Finally, for the case of excitation by a shear moment it has appeared that for the particular set of parameters considered here, the energy input ($\bar{N}_{input} = 0{\cdot}00275$) depends very weakly on the depth parameter and all the power is transmitted through the plate, while participation of the acoustical path is negligibly small. The absence of the acoustical power flow is explained by a rather weak interaction between shear and transverse motions of the plate having a very soft core ply. Therefore, the structural dominantly shear mode does not produce large lateral motions of a sandwich plate and it generates a weak acoustic field.

All the results reported in this section are obtained for an infinitely long homogeneous plate. In practice, it is more realistic to deal with a plate connected to some other structures. At the junction points, the interaction of various modes may result in re-distribution of the energy flows between the plate and the fluid. This aspect is addressed in the following section of the paper.

5. VIBRATIONS OF AND ENERGY FLOWS IN A FLUID-LOADED SANDWICH PLATE WITH TWO IDENTICAL INCLUSIONS

As is known for the case of vibrations of an infinitely long sandwich plate without fluid loading (see reference [3]), inclusions significantly distort its shape of vibrations. In this part of the paper, the role of two identical inclusions in the energy transportation through a sandwich plate in heavy fluid loading conditions is considered. The forced vibrations of an infinitely long sandwich plate may then be associated with the resonant behaviour typical to the trapped mode effect, and this will be investigated now.

Let two identical inclusions of mass M_0 supported by linear springs of the same stiffness K_0 be placed at the points x_1, x_2. The distance between these points is denoted as $l = x_2 - x_1$. Assume for simplicity that these inclusions do not produce inertial forces and moments in response to shear and rotational displacements and that the springs resist only vertical displacements. A driving generalized force (a concentrated transverse force, a concentrated bending moment, or a concentrated shear moment) of the unit amplitude and the frequency ω acts at the point $x = x_0$. The Green functions obtained in section 3 formulate the shape of vibrations of a sandwich beam with no inclusion in all these cases. The equation of motions of each mass is formulated as

$$-M_0\omega^2 w_j = R_j - K_0 w_j, \quad j = 1, 2, \tag{22}$$

while the amplitude of a displacement of the plate at an arbitrary point is given by

$$w(x) = F_{0n} W_n(x, x_0) - R_1 W_1(x, x_1) - R_2 W_1(x, x_2). \tag{23}$$

In equation (23), $F_{0n} = 1$ is a driving concentrated force of the unit amplitude for $n = 1$, a driving concentrated bending moment for $n = 2$ or a driving concentrated shear moment for $n = 3$. This equation is equally applicable to all these excitation cases. Respectively, functions W_n, $n = 1, 2, 3$ are the components of the Green matrix formulating a lateral displacement in response to a force or to moments respectively. Note that forces R_1, R_2 act vertically downwards on the plate, leading to the minus sign in equation (11).

The continuity conditions at $x = x_j$, $j = 1, 2$ give the following system of linear algebraic equations for the amplitudes of displacements of the concentrated masses:

$$\left[1 + \kappa\left(1 - \frac{\omega^2}{\omega_0^2}\right) W_1(x_1, x_1)\right] w(x_1) + \kappa\left(1 - \frac{\omega^2}{\omega_0^2}\right) W_1(x_2, x_1) w(x_2) = f_{0n} W_n(x_1, x_0),$$

$$\kappa\left(1 - \frac{\omega^2}{\omega_0^2}\right) W_1(x_1, x_2) w(x_1) + \left[1 + \kappa\left(1 - \frac{\omega^2}{\omega_0^2}\right) W_1(x_2, x_2)\right] w(x_2) = f_{0n} W_n(x_2, x_0). \tag{24}$$

Here, $\omega_0 = \sqrt{K_0/M_0}$ is the eigenfrequency of the isolated mass supported by the spring, and $\kappa = K_0 h^2/D$ is the non-dimensional stiffness of the attachment. If $n = 1$, then a concentrated force is applied, and the non-dimensional parameter of a force is $f_{01} = F_{01}/Eh$. If $n = 2$ or 3, then a concentrated moment is applied and the non-dimensional parameter of a moment is $f_{0n} = F_{0n}/Eh^2$.

Then, the shape of forced vibrations of the sandwich beam becomes

$$w(x) = f_{0n}\left[W_n(x, x_0) - \kappa\left(1 - \frac{\omega^2}{\omega_0^2}\right) W_1(x_1, x) w(x_1) - \kappa\left(1 - \frac{\omega^2}{\omega_0^2}\right) W_1(x_2, x) w(x_2)\right]. \tag{25a}$$

Respectively, a shear angle at an arbitrary cross-section of the sandwich plate is formulated as

$$\theta(x) = f_{0n}\left[\Theta_n(x, x_0) - \kappa\left(1 - \frac{\omega^2}{\omega_0^2}\right)\Theta_1(x_1, x)w(x_1) - \kappa\left(1 - \frac{\omega^2}{\omega_0^2}\right)\Theta_1(x_2, x)w(x_2)\right]. \tag{25b}$$

It follows from equations (24) that a plate may perform vibrations trapped between two masses when the determinant of this system of linear algebraic equations is zero: i.e.,

$$\left[1 + \kappa\left(1 - \frac{\omega^2}{\omega_0^2}\right)\sum_{j=1}^{M} \bar{W}_{1j}\right]^2 - \kappa^2\left(1 - \frac{\omega^2}{\omega_0^2}\right)^2\left(\sum_{j=1}^{M} \bar{W}_{1j}\exp(K_j|x_1 - x_2|)\right)^2 = 0. \tag{26}$$

The wave numbers $K_j, j = 1, 2, \ldots, M$ and the coefficients $\bar{W}_j, j = 1, 2, \ldots, M$ are frequency dependent as specified by equations (9) and (14) so that this equation may be solved numerically.

The set of parameters of a water-loaded sandwich plate is taken to be the same as in previous sections, the excitation frequency is $\Omega = 0{\cdot}01$, the other parameters are $\kappa = 10$, $\omega/\omega_0 = 0{\cdot}5$. In Figure 5, the energy flows propagating to the left and to the right from the excitation point through the structure are presented by curves 1 and 2, the energy flows propagating to the left and to the right from the excitation point through the acoustic medium are presented by curves 3 and 4. The concentrated transverse force is located at $x = 0$, inclusions are positioned at $x_1 = 100h$ and $x_2 = 200h$. As is seen, the presence of two inclusions results in complete isolation of the "outer" part of a sandwich plate to the right from inclusions from the energy flow. All power input is actually channelled to the homogeneous part of the plate to the left from the excitation point and most of the energy is transported by the structure. In fact, since the energy flow is directed to the left, it has the negative sign. Thus, in Figure 5 the energy flows for $x > 0$ are taken with their own signs, while energy flows for $x < 0$ are for convenience taken with opposite signs.

To explore the effect of trapped mode vibrations for a plate of the same set of parameters, it is necessary to plot a dependence of the determinant (26) on the distance between inclusions. It is convenient to have the position of the first inclusion fixed at, say, $x_1 = 100h$ and to use as an independent variable the co-ordinate of the second point. This dependence is shown in Figure 6. The real part of the determinant, its imaginary part and module are presented by curves 1, 2 and 3 respectively. The first resonant frequency is relevant to the location of the second inclusion at $x_2 = 116{\cdot}5h$. The second one is relevant to its location at $x_2 = 133h$. In fact, such a short distance between inclusions is fairly close to the limit of validity range of the theory of sandwich plates adopted here. This also justifies a choice of $\Omega = 0{\cdot}01$ for the anaysis of dispersion curves performed in section 2 of this paper.

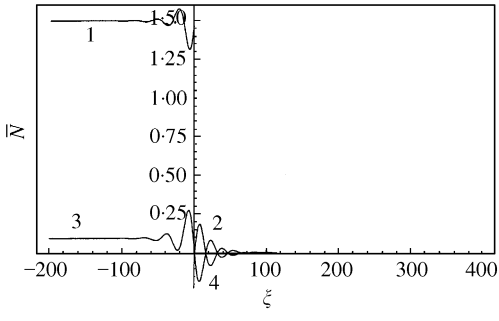

Figure 5. Energy flows in a plate with two inclusions loaded by a transverse force, $\Omega = 0{\cdot}01$, $\chi = 10$.

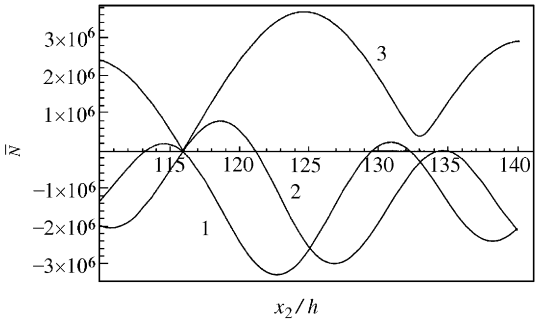

Figure 6. Frequency determinant versus position of the second inclusion at $\Omega = 0{\cdot}01$, $\chi = 10$.

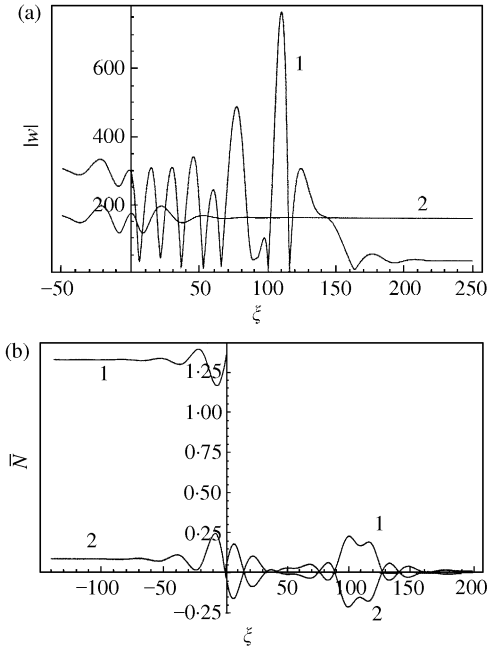

Figure 7. Mode trapping at the first resonant case, transverse excitation; (a) absolute values of amplitudes of vibrations; and (b) energy flows.

In Figure 7(a), the absolute value of a displacement is plotted versus an axial co-ordinate in the case, when $x_1 = 100h$, $x_2 = 116{\cdot}5h$ by curve 1. Curve 2 displays the absolute value of a displacement of the plate with no inclusions. It is interesting to note that to the left of the excitation point, the amplitude of vibrations of a homogeneous plate is approximately 2 times smaller than the amplitude of vibrations of a plate with two inclusions. There is a sharp peak of the amplitude of a supported plate between inclusions, that is physically explained by mode trapping. The amplitude of vibrations is also rather large between the excitation point and the first inclusion and within a certain distance from the right inclusion (approximately up to $x = 160h$). Further to the right, the amplitude of displacement of a supported plate is much smaller, than that of a homogeneous one. These results provide an explanation for the pattern of energy flows shown in Figure 7(b). To the left from $x = 0$, the picture is qualitatively the same as the one shown in Figure 5. It is more interesting to

look at the energy flows to the right from the excitation point. The energy flow through the structure (curve 1) is oscillating and so is the acoustic energy flow. It is remarkable, however, that the sum of these two components is maintained on balance fairly close to zero. At around $x = 160h$, each of these components reaches a certain value which does not vary with further growth in x. The presence of the negative energy flows through the acoustic medium constitutes a physical mechanism of localization of vibrations of a plate (the resonant mode trapping).

A character of mode trapping discussed for the first resonant frequency is quite different from the one found for the second resonant frequency. In Figure 8(a), the absolute value of a displacement is plotted versus an axial co-ordinate in the case, when $x_1 = 100h$, $x = 133h$ by curve 1. Curve 2 displays the shape of vibrations of a plate with no inclusions. It is interesting to note that everywhere except for the interval $50h < x < 250h$, the amplitude of vibrations of a homogeneous plate is approximately the same as the amplitude of vibrations of a plate with two inclusions. The resonant mode trapping manifests itself by two sharp peaks of the amplitude of a supported plate between inclusions, see also Figure 8(b) which displays the zoomed part of Figure 8(a). Such a shape is relevant to the skew-symmetric mode of vibrations. A dependence of components of the energy flow on an axial co-ordinate is shown in Figure 8(c). The energy flows propagating to the left and to the right from the excitation point through the structure are presented by curves 1 and 2, the energy flows propagating to the left and to the right from the excitation point through the acoustic medium are presented by curves 3 and 4. As is seen, in these excitation conditions, mode trapping does not prevent propagation of the energy to the right from the excitation point in the same amount as to the left. The multiple short circuits in this case are arranged in such a manner, that the mean energy flow at any cross-section $x > 0$ remains the same and equal to half of the energy input. The case considered here is relevant to the absence of free propagating acoustic modes, i.e., the excitation frequency is beyond its cut-on value.

In the case, where in addition to the propagating structural modes there is also the propagating acoustic one, it is sufficient to put $\chi = 50$. In this case, frequency determinant (26) depends on the position of the second inclusion as is shown in Figure 9(a). Its real part, its imaginary part and its absolute value are designated by curves 1, 2 and 3 respectively. The first minimum of curve 3 is reached at $x_2 = 130{\cdot}9h$. In Figure 9(b), the absolute value of the amplitude of a displacement is plotted versus an axial co-ordinate in the case, when $x_1 = 100h$, $x_2 = 130{\cdot}9h$ by curve 1. Curve 2 displays the absolute value of the amplitude of a displacement of the plate with no inclusions. This graph is quite similar to the one displayed in Figure 7(a), but there is also a difference which can be explained by excitation at a frequency above the cut-on one. In a far field, there is a harmonic fluctuation of the amplitude of vibrations around some mean value. In Figure 9(c), the energy flows propagating to the left and to the right from the excitation point through the structure are presented by curves 1 and 2, the energy flows propagating to the left and to the right from the excitation point through the acoustic medium are presented by curves 3 and 4. The energy propagation to the left is almost the same as in the case of a homogeneous sandwich plate; see Figure 2(c). The levels of the energy flows in the structure and in the fluid are approximately the same in the region between the excitation point and inclusions and also in the zone between inclusions. Their pattern is rather complicated there, but it is remarkable that the energy flow emerging from the zone with inclusions to the right is composed mostly by the acoustic part, rather than by the structural one. As is seen in Figure 9(c), the negative energy flow in the structure between inclusions enhances the acoustic energy flow. It should also be pointed out that the amplitude of vibrations between inclusions is smaller in this case than in a case when there are no fluid-dominated propagating modes.

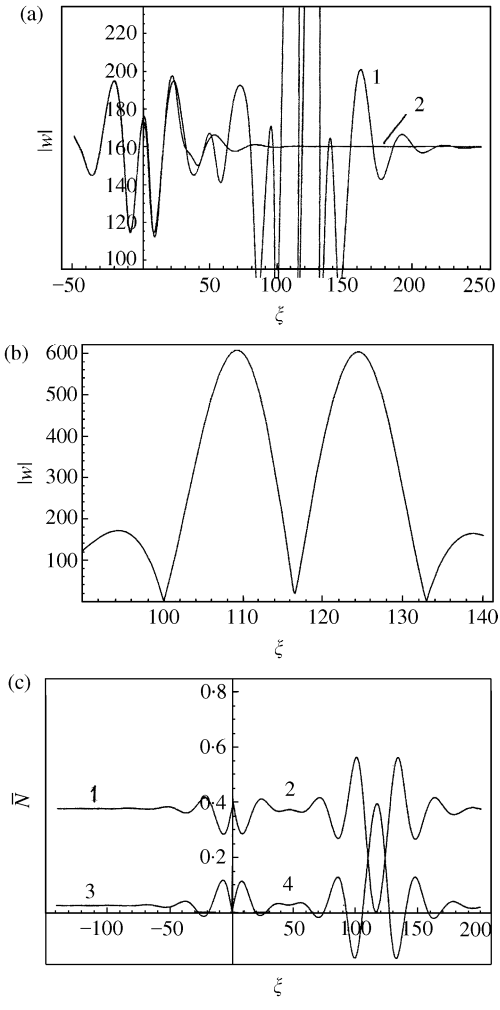

Figure 8. Mode trapping at the second resonant case, transverse excitation, $\Omega = 0{\cdot}01$, $\chi = 10$: (a) absolute values of amplitudes of vibrations; (b) absolute values of amplitudes of vibrations between inclusions; and (c) energy flows.

The dynamics of a fluid-loaded sandwich plate with two inclusions is influenced by several parameters. In particular, the roles of the depth parameter χ and the frequency parameter Ω are linked to each other as has been discussed in respect to the dispersion relation. The roles of stiffness and inertial characteristics of inclusions are similar to those in the case of a plate with no fluid loading, see reference [3], and they are not explored any further. For brevity, instead of a parametric study of vibrations excited by a point transverse force, vibrations of a plate loaded by a concentrated moment are briefly studied. All parameters of the sandwich plate composition and parameters of inclusions are kept the same, fluid loading is produced by a water layer of $\chi = 10$, the driving unit bending moment is applied at $x = 0$, the excitation frequency is $\Omega = 0{\cdot}01$. The first inclusion is located at $x_1 = 100h$. The second inclusion is put at $x_2 = 116{\cdot}9h$. In Figure 10(a), the absolute value of the amplitude of lateral vibrations of a plate with inclusions versus an axial coordinate x is shown by curve 1, the shape of vibrations of a plate without inclusions is illustrated by curve 2. It is seen that although localization phenomenon still exists, the maximum amplitude

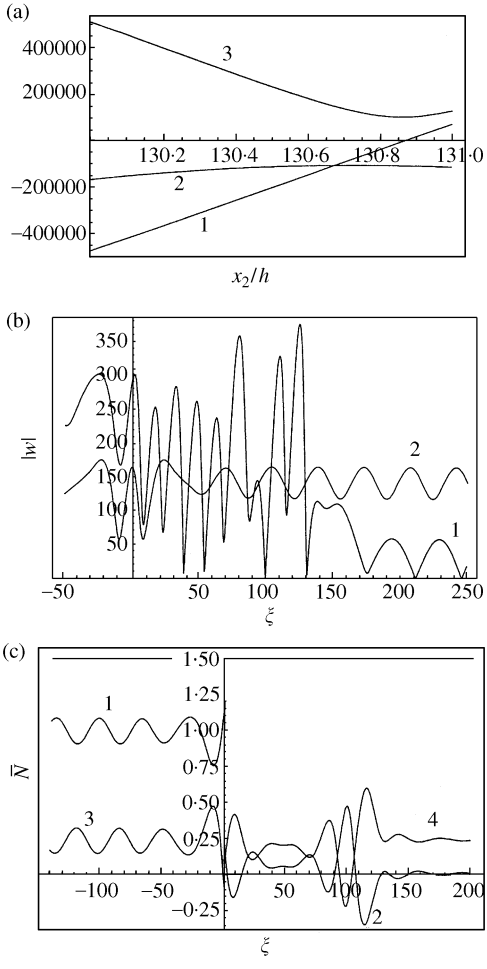

Figure 9. Mode trapping at $\Omega = 0{\cdot}01$, $\chi = 10$, transverse excitation, $\Omega = 0{\cdot}01$, $\chi = 10$: (a) frequency determinant versus position of the second inclusion; (b) absolute values of amplitudes of vibrations; and (c) energy flows.

between inclusions is much smaller than that in the case of transverse excitation. This is explained by the large difference between elastic modules of skin and core plies, $\gamma = 0{\cdot}0001$. The curves in Figure 10(b) are plotted for the same parameters, but the second inclusion is located at $x_2 = 133h$. Such a distance between inclusions is relevant to the second resonance of a plate as is confirmed by curve 1 plotted for a plate with inclusions. Apparently, curves 2 in Figures 10(a, b) display the same shape of vibrations. The energy flow in both these cases is almost exactly the same as in the case of a homogeneous plate; see the discussion in section 4. Finally, in the case of a shear excitation, the role of inclusions is insignificant and the energy is transported only in the structure as also has been discussed in section 4.

6. CONCLUSIONS

A complete investigation has been presented of stationary vibrations of an infinitely long sandwich plate in contact with a layer of an ideal compressible fluid. The analysis of

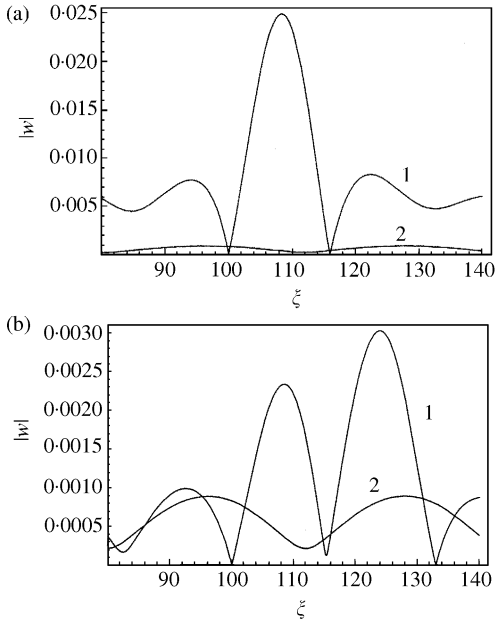

Figure 10. Mode trapping at $\Omega = 0{\cdot}01$, $\chi = 10$, excitation by a bending moment; (a) the first resonant case; and (b) the second resonant case.

dependence of roots of the dispersion equation on the frequency parameter and on the depth parameter is performed. Then, elements of the Green matrix describing the response of a plate to the point loading by a transverse force or by moments are constructed analytically as linear combinations of the normal modes. Formulation of the response of a fluid-loaded structure by the Green matrix is truncated to a finite number of these modes and a convergence rate is estimated. For a sandwich plate with no inclusions, the analysis of the energy flows is performed by the direct use of the Green matrix. Excitation by a point force and by point moments is considered. It is found that the distribution of the input power between the "structural" transmission path and the "acoustic" transmission path is strongly affected by the frequency parameter and the "depth" parameter. Specifically, these parameters control not only the proportion between the energy flow in the structure and in the fluid, but also the length of a nearfield zone. It is found that for a sandwich plate with a very soft core ply, excitation by a shear motion does not produce large energy flow in the fluid. Then, the case of forced vibrations of an infinitely long fluid-loaded sandwich plate with two identical inclusions is considered. The phenomenon of trapping of the flexural modes is explored. For each particular set of parameters a spectrum of "resonant" distances between inclusions is detected, when strongly localized large amplitude vibrations are generated by a transverse point force applied at a sufficiently large distance from the span between inclusions. It is found that the energy flows in the structure and in the fluid are strongly affected by the presence of these inhomogeneous. In particular, the energy flows either in the structure or in the fluid directed towards the excitation point are detected at certain distances from the point. The pattern of distribution of the energy flows creates a mechanism for trapped modes generation. It is also shown that a trapped mode may produce a screening phenomenon and prevent energy propagation beyond inclusions. Finally, in the case of a shear excitation, it is found that inclusions responding to transverse motions do not affect the energy propagation in sandwich plates with a soft core.

REFERENCES

1. V. R. SKVORTSOV 1993 *Transactions of the Academy of Sciences of Russia, Mechanics of a Rigid Body* **1**, 162–168. Symmetrically inhomogeneous through thickness plate as a sandwich plate having a soft core (in Russian).
2. S. V. SOROKIN 2000 *International Journal of Composite Structures* **48**, 219–230. Vibrations of and sound radiation from sandwich plates in heavy fluid loading conditions.
3. S. V. SOROKIN and N. PEAKE 2000 *Journal of Sound and Vibration* **237**, 203–220. Vibrations of sandwich panels with concentrated masses and spring-like inclusions.
4. N. PEAKE and S. V. SOROKIN 2001 *Journal of Sound and Vibration* **242**, 597–617. On the behaviour of fluid-loaded sandwich panels with mean flow.
5. V. SHROTER and F. J. FAHY 1981 *Journal of Sound and Vibration* **74**, 465–476. Point-force excited vibrations of a thin, infinite plate separating a fluid layer from a fluid half-space.
6. D. G. CRIGHTON and D. INNES 1984 *Philosophical Transactions of the Royal Society of London, Series* A **312**, 295–341. The modes, resonances and forced response of elastic structures under heavy fluid loading.
7. M. JUNGER and D. FEIT 1993 *Sound, Structures and their Interaction*. Cambridge, Massachusetts: MIT Press.
8. L. YA. GUTIN 1964 *Akusticheskij Zhurnal* **10**, 431–434. Sound radiation by an unbounded plate excited by a point load (in Russian).
9. F. FAHY 1990 *Sound and Structural Vibration*: *Radiation, Transmission and Response*. London: Academic Press.
10. C. R. FULLER and F. J. FAHY 1982 *Journal of Sound and Vibration* **81**, 501–518. Characteristics of wave propagation and energy distribution in cylindrical elastic shells filled with fluid.
11. C. R. FULLER 1983 *Journal of Sound and Vibration* **87**, 409–427. The input mobility of an infinite circular cylindrical elastic shell filled with fluid.
12. S. V. SOROKIN, J. BALLE NIELSEN and N. OLHOFF 2001 *Journal of Structural and Multidisciplinary Optimisation* **22**, 3–23. Boundary equations method for analysis of vibrations and energy flows in cylindrical shells without fluid and in fluid-loaded cylindrical shells.
13. D. V. EVANS and C. M. LINTON 1991 *Journal of Fluid Mechanics* **225**, 153–175. Trapped modes in open channels.
14. D. A. INDEJTSEV 1995 *Journal of Technical Acoustics* **2**, 123–142. Trapped modes in elastic systems with inclusions.
15. D. ZENKERT 1995 *An Introduction to Sandwich Construction*. London: EMAS Ltd.
16. S. P. TIMOSHENKO 1955 *Vibration Problems in Engineering*. Toronto: D. Van Nostrand Co.
17. H. G. ALLEN 1969 *Analysis and Design of Structural Sandwich Panels*. Oxford: Pergamon Press.
18. S. WOLFRAM 1991 *Mathematica*: *A System for Doing Mathematics by Computer*. Reading, Massachusetts: Addison-Wesley Publishing Co.